Cell Metabolism, Volume *15*

Supplemental Information

Fumarate Is Cardioprotective via Activation of the Nrf2 Antioxidant Pathway

Houman Ashrafian, Gabor Czibik, Mohamed Bellahcene, Dunja Aksentijević, Anthony C. Smith, Sarah J. Mitchell, Michael S. Dodd, Jennifer Kirwan, Jonathan J. Byrne, Christian Ludwig, Henrik Isackson, Arash Yavari, Nicolaj B. Støttrup, Hussain Contractor, Thomas J. Cahill, Natasha Sahgal, Daniel R. Ball, Rune I.D. Birkler, Iain Hargreaves, Daniel A. Tennant, John Land, Craig A. Lygate, Mogens Johannsen, Rajesh K. Kharbanda, Stefan Neubauer, Charles Redwood, Rafael de Cabo, Ismayil Ahmet, Mark Talan, Ulrich L. Günther, Alan J. Robinson, Mark R. Viant, Patrick J. Pollard, Damian J. Tyler, and Hugh Watkins

Table S1 related to Figure 4

Results for FT-ICR mass spectrometry metabolomics

List of putative identities based on the mass spectrometry data of the top 350 discriminant peaks between wild type and Fh -/- mouse cardiac biopsies. Peaks were selected by a PLS-DA forward-selection approach based on minimising the classification error. Only peaks that could be ascribed an identity are displayed.

Observed		Statistics			Identification							
m/z	Average intensity	Fold change[a]	LV weights[b]	LV weights by rank	No. of empirical formulae	No. of metabolite names	Empirical formula	Theoretical mass (metabolite) (Da)	Ion form	Theoretical mass (Da) (in adduct form)	Mass error (ppm)	Putative metabolite name(s)
347.03981	290510.7	-2.65	0.159991	2	24	1	C10H13N4O8P	348.04710	[M-H]-	347.03983	-0.05	IMP
384.99549	32744.2	-2.75	0.157639	4	46	1	C10H13N4O8P	348.04710	[M+K-2H]-	384.99571	-0.57	IMP
369.02188	24248.8	-2.55	0.133747	7	33	1	C10H13N4O8P	348.04710	[M+Na-2H]-	369.02177	0.29	IMP
214.99643	23423.5	+1.74	-0.10522	11	5	1	C4H9O8P	216.00351	[M-H]-	214.99623	0.92	4-Phospho-D-erythronate
236.97832	13917.1	+1.95	-0.10164	15	5	1	C4H9O8P	216.00351	[M+Na-2H]-	236.97818	0.61	4-Phospho-D-erythronate
252.95225	21512.6	+1.69	-0.09472	19	7	1	C4H9O8P	216.00351	[M+K-2H]-	252.95211	0.54	4-Phospho-D-erythronate
357.08906	8908.6	-1.84	0.076809	42	18	1	C12H22N2O6S	322.11986	[M+Cl]-	357.08926	-0.56	N-((R)-Pantothenoyl)-L-cysteine
						1	C11H23N2O7PS	358.09636	[M-H]-	357.08909	-0.07	Pantetheine 4-phosphate
313.04432	7274.9	+1.98	-0.07467	46	14	1	C8H15N2O9P	314.05152	[M-H]-	313.04424	0.24	5-Phosphoribosyl-N-formylglycinamide
558.06452	248667.7	-1.55	0.074656	47	149	2	C15H23N5O14P2	559.07168	[M-H]-	558.06440	0.21	ADP-ribose, Phosphoribosyl-AMP
279.03891	16402.7	-1.46	0.064229	62	11	1	C10H14N2O5	242.09027	[M+K-2H]-	279.03888	0.11	Thymidine
						2	C9H12N2O6	244.06954	[M+Cl]-	279.03894	-0.11	Pseudouridine, Uridine
243.06234	52764	-1.36	0.063534	66	3	2	C9H12N2O6	244.06954	[M-H]-	243.06226	0.32	Pseudouridine, Uridine
243.02760	29580.7	-1.39	0.05497	102	7	1	C11H10O5	222.05283	[M+Na-2H]-	243.02749	0.44	2-Succinylbenzoate

Observed		Statistics			Identification							
m/z	Average intensity	Fold change[a]	LV weights[b]	LV weights by rank	No. of empirical formulae	No. of metabolite names	Empirical formula	Theoretical mass (metabolite) (Da)	Ion form	Theoretical mass (Da) (in adduct form)	Mass error (ppm)	Putative metabolite name(s)
						3	C6H13O8P	244.03481	[M-H]-	243.02753	0.28	L-Fucose 1-phosphate, L-Fuculose 1-phosphate, L-Rhamnulose 1-phosphate
580.04646	31239	-1.36	0.051448	122	193	2	C15H23N5O14P2	559.07168	[M+Na-2H]-	580.04635	0.19	ADP-ribose, Phosphoribosyl-AMP
353.21002	13978.8	-1.92	0.04822	135	7	5	C21H32O3	332.23515	[M+Na-2H]-	353.20981	0.58	17alpha,20alpha-Dihydroxypregn-4-en-3-one, 17alpha-Hydroxypregnenolone, 21-Hydroxypregnenolone, 5alpha-Dihydrodeoxycorticosterone, 7alpha-Hydroxypregnenolone
465.30436	108682.4	-2	0.046713	147	10	1	C27H46O4S	466.31168	[M-H]-	465.30441	-0.1	Cholesterol sulphate
215.05380	3402.3	+2.29	-0.04664	148	3	3	C7H14O6	194.07904	[M+Na-2H]-	215.05371	0.43	1-O-Methyl-myo-inositol, 3-O-Methyl-myo-inositol, Methyl beta-D-galactoside
303.08358	5996.6	-1.52	0.041644	172	10	1	C11H16N2O8	304.09067	[M-H]-	303.08339	0.62	N-Acetyl-aspartyl-glutamate
281.03594	4244.7	-1.71	0.037522	193	8	2	C9H12N2O6	244.06954	[M+(37Cl)]-	281.03599	-0.18	Pseudouridine, Uridine
193.07189	4300.1	+1.7	-0.03713	198	2	3	C7H14O6	194.07904	[M-H]-	193.07176	0.65	1-O-Methyl-myo-inositol, 3-O-Methyl-myo-inositol, Methyl beta-D-galactoside
201.01717	4699.2	+1.61	-0.03683	202	3	6	C6H12O5	164.06848	[M+K-2H]-	201.01708	0.44	6-Deoxy-L-galactose, D-Rhamnose, L-Fuculose, L-Rhamnofuranose, L-Rhamnose, L-Rhamnulose
						4	C5H10O6	166.04774	[M+Cl]-	201.01714	0.14	D-Xylonate, L-Arabinonate, L-Lyxonate, L-Xylonate

Observed		Statistics			Identification							
m/z	Average intensity	Fold change[a]	LV weights[b]	LV weights by rank	No. of empirical formulae	No. of metabolite names	Empirical formula	Theoretical mass (metabolite) (Da)	Ion form	Theoretical mass (Da) (in adduct form)	Mass error (ppm)	Putative metabolite name(s)
306.08061	2407	-1.88	0.034391	218	9	3	C15H17NO4S	307.08783	[M-H]-	306.08055	0.18	(1R)-Hydroxy-(2R)-N-acetyl-L-cysteinyl-1,2-dihydronaphthalene, (1R)-N-Acetyl-L-cysteinyl-(2R)-hydroxy-1,2-dihydronaphthalene, (1S)-Hydroxy-(2S)-N-acetyl-L-cysteinyl-1,2-dihydronaphthalene
175.02493	31703.5	+1.14	-0.03323	223	1	6	C6H8O6	176.03209	[M-H]-	175.02481	0.67	(4S)-4,6-Dihydroxy-2,5-dioxohexanoate, 2-Hydroxy-3-oxoadipate, 5-Dehydro-4-deoxy-D-glucuronate, Ascorbate, D-Glucuronolactone, L-xylo-Hexulonolactone
564.06350	11878.2	+1.3	-0.03266	227	164	1	C15H25N3O16P2	565.07101	[M-H]-	564.06374	-0.42	CDP-glucose
479.97316	16190.9	+1.21	-0.03202	228	119	1	C10H15N5O11P2	443.02434	[M+K-2H]-	479.97294	0.45	GDP
442.01697	50664.4	+1.17	-0.03178	229	65	1	C10H15N5O11P2	443.02434	[M-H]-	442.01706	-0.2	GDP
438.00879	10036.1	+1.24	-0.02759	254	63	1	C10H17N3O11P2	417.03384	[M+Na-2H]-	438.00851	0.65	2-Deoxy-5-hydroxymethylcytidine-5-diphosphate
215.03290	110550.9	-1.08	0.022441	274	4	15	C6H12O6	180.06339	[M+Cl]-	215.03279	0.5	D-Allose, D-Fructose, D-Fuconate, D-Galactose, D-Glucose, D-Mannose, D-Tagatose, L-Galactose, L-Gulose, L-Rhamnonate, L-Sorbose, alpha-D-Glucose, beta-D-Fructose, beta-D-Glucose, myo-Inositol

Observed		Statistics			Identification							
m/z	Average intensity	Fold change[a]	LV weights[b]	LV weights by rank	No. of empirical formulae	No. of metabolite names	Empirical formula	Theoretical mass (metabolite) (Da)	Ion form	Theoretical mass (Da) (in adduct form)	Mass error (ppm)	Putative metabolite name(s)
217.02996	33471	-1.09	0.022117	278	2	15	C6H12O6	180.06339	[M+(37Cl)]-	217.02984	0.55	D-Allose, D-Fructose, D-Fuconate, D-Galactose, D-Glucose, D-Mannose, D-Tagatose, L-Galactose, L-Gulose, L-Rhamnonate, L-Sorbose, alpha-D-Glucose, beta-D-Fructose, beta-D-Glucose, myo-Inositol
424.97667	18546	+1.07	-0.0199	291	65	1	C9H14N2O12P2	404.00220	[M+Na-2H]-	424.97687	-0.48	UDP
378.24158	34010.8	-1.15	0.017431	302	7	1	C18H38NO5P	379.24876	[M-H]-	378.24149	0.25	Sphingosine 1-phosphate
402.99490	45957.8	-1.08	0.013251	320	57	1	C10H13N2O11P	368.02570	[M+Cl]-	402.99510	-0.5	Orotidine 5-phosphate
						1	C9H14N2O12P2	404.00220	[M-H]-	402.99493	-0.07	UDP
440.95101	15715.4	+1.05	-0.01215	322	102	1	C9H14N2O12P2	404.00220	[M+K-2H]-	440.95081	0.45	UDP
174.08853	23845	-1.13	0.011894	323	1	1	C6H13N3O3	175.09569	[M-H]-	174.08842	0.66	L-Citrulline
174.04091	7137.2	-1.17	0.011671	326	1	2	C6H9NO5	175.04807	[M-H]-	174.04080	0.65	N-Acetyl-L-aspartate, N-Formyl-L-glutamate
402.01076	17037.2	-1.07	0.010535	330	46	1	C9H15N3O11P2	403.01819	[M-H]-	402.01091	-0.38	CDP
253.09295	16051.9	-1.04	0.000864	349	4	2	C9H18O8	254.10017	[M-H]-	253.09289	0.22	2-(beta-D-Glucosyl)-sn-glycerol, 3-beta-D-Galactosyl-sn-glycerol

a) fold change in concentration of compound in knock out compared to wild type
b) LV1 weights from a PLS-DA model built from variables that had been forward selected based on regression values to maximise the separation between groups

Table S2 related to Figure 4
Summary of the most upregulated and downregulated genes in the microarray

Gene ID	*Gene name*	*Fold change*
ITGB1BP3	nicotinamide riboside kinase 2	4.85 ↑
MTHFD2	methylenetetrahydrofolate dehydrogenase (NAD+ dependent), methenyltetrahydrofolate cyclohydrolase	4.36 ↑
GDF15	growth differentiation factor 15	4.07 ↑
ASNS	asparagine synthetase	3.17 ↑
GSTA1	glutathione S-transferase, alpha 1	2.78 ↑
GSTA2	glutathione S-transferase alpha 2	2.32 ↑
AQP8	aquaporin 8	2.05 ↑
SCN4B	sodium channel, type IV, beta	2.04 ↑
RNF30	tripartite motif-containing 54	1.59 ↑
NQO1	NAD(P)H dehydrogenase, quinone 1	1.50 ↑
ATF5	activating transcription factor 5	1.49 ↑

UPP1	uridine phosphorylase 1	1.48 ↑
UCHL3	ubiquitin carboxyl-terminal esterase L3	1.41 ↑
GSTO1	glutathione S-transferase omega 1	1.34 ↑
VIM	vimentin	1.27 ↓
TKT	transketolase	1.32 ↓
KCNJ3	potassium inwardly-rectifying channel, subfamily J, member 3 (K_{ir}3.1)	1.52 ↓
AQP4	aquaporin 4	1.70 ↓
HIST1H2AH	histone cluster 1, H2ah	1.80 ↓
PPP1R1B	protein phosphatase 1, regulatory (inhibitor) subunit 1B	1.86 ↓
TNNI2	troponin I, fast skeletal muscle	1.92 ↓
MYL4	myosin light chain 4	4.09 ↓
MYL7	myosin light chain 7	4.88 ↓
SLN	sarcolipin	5.22 ↓

Figure S1 related to Figures 2 and 4

Gene expression of HIF-α regulators and targets (A) and Keap1 (B). White: control, black: Fh1 KO; n=5/group, * $p<0.05$.

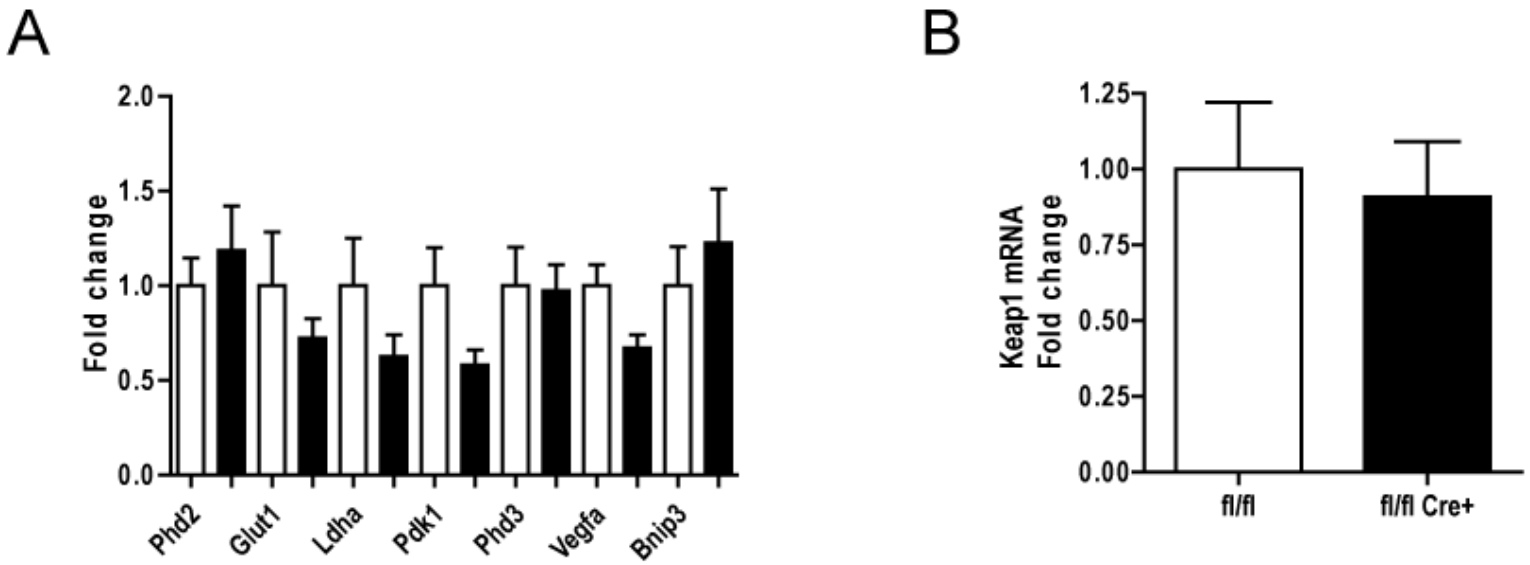

Figure S2 related to Figure 2

A mass spectrometry based metabolomics approach, detected 6303 separate peaks and revealed substantial differences in the metabolic profiles of the Fh1 KO compared to control hearts as evidenced by the scores plot from the analysis of negative ion FT-ICR mass spectra of cardiac tissue Fh1-/- (▼) and control (●) mice. A forward selection strategy revealed 350 of these 6303 mass spectral peaks maximally discriminated Fh1 KO vs WT hearts in the PLS-DA model (average classification error of 2.1%; p<0.0001). Empirical formula(e) assigned to these 350 peaks were mapped onto pathways listed in the KEGG database to assess which pathways had been most affected (see Supp Table.1).

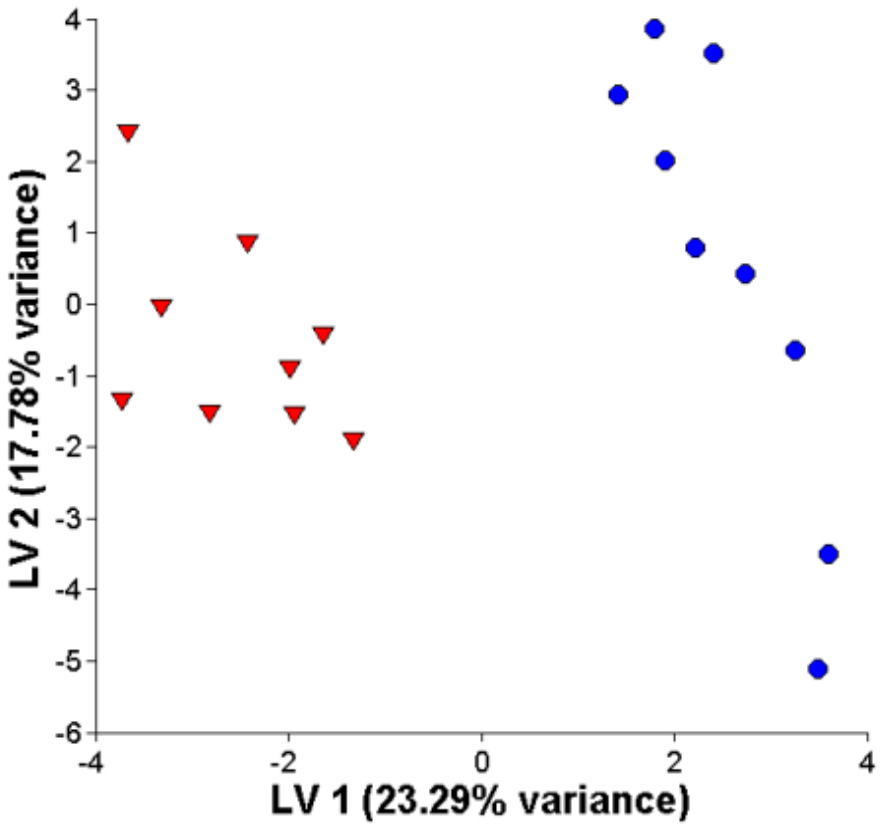

Figure S3 related to Figure 4

A depiction of myocardial metabolism under normal conditions as derived from simulations.

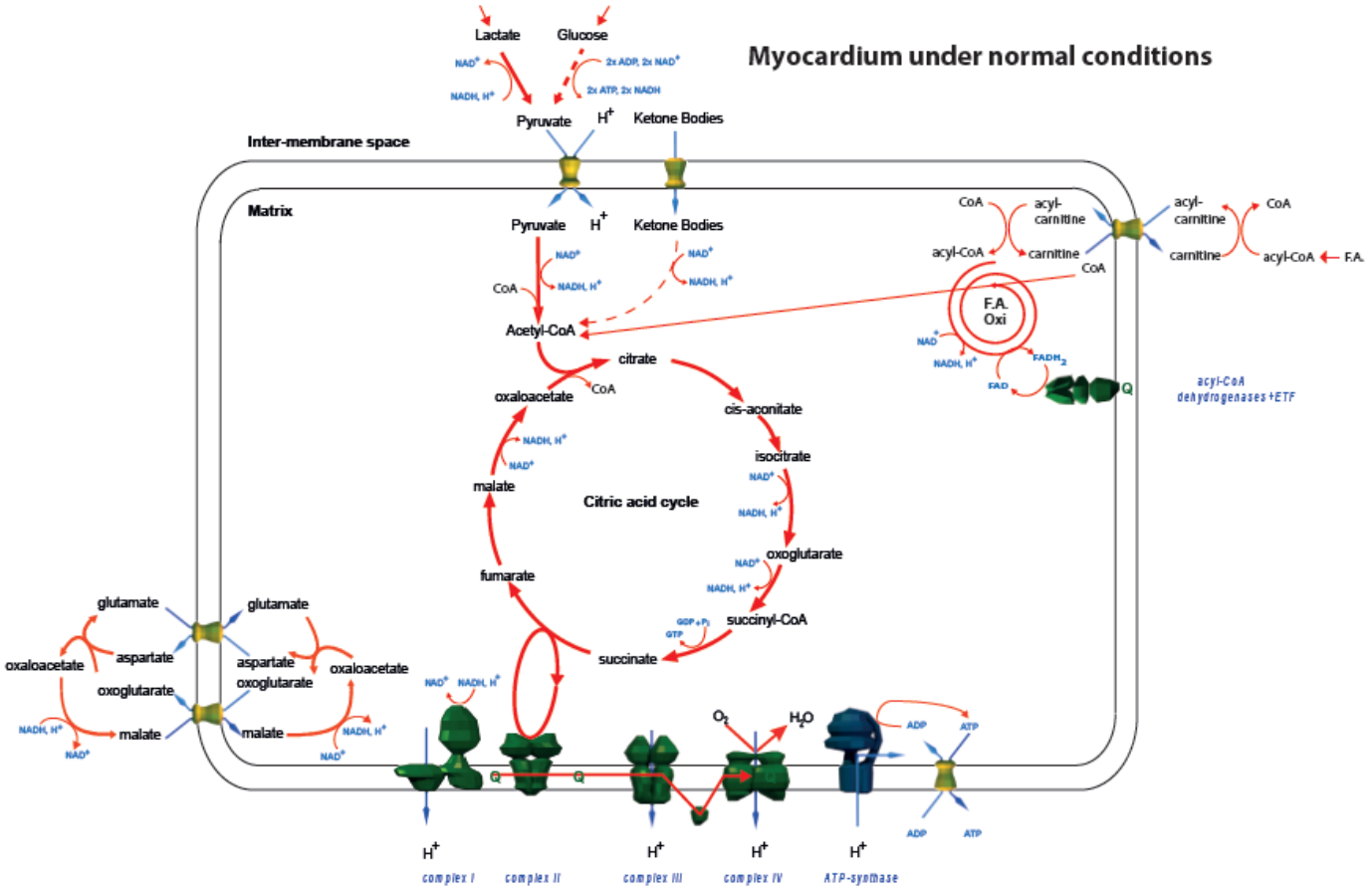

Figure S4 related to Figure 4

Hyperpolarized ^{13}C label studies to assess label incorporation into intermediary metabolites. Left panel: Representative spectrum acquired from a mouse heart in vivo after infusion of hyperpolarized [2-13C]pyruvate. 3 seconds of data were summed, and a line broadening of 15 Hz was applied. This metabolic tracer has enabled dynamic in vivo assessment of the first span of the Krebs cycle. For illustrative purposes it is important to note that while the citrate peak is small, the glutamate peak is broad but and visible above the noise hence more optimally analysed. Right Panel.A summary of the metabolic fate of infused [1-13C]pyruvate and [2-13C]pyruvate. White: control, black: Fh1 KO; for lactate, bicarbonate and alanine n=8-9/group, for citrate, glutamate and acetylcarnitine n=4-5.

.

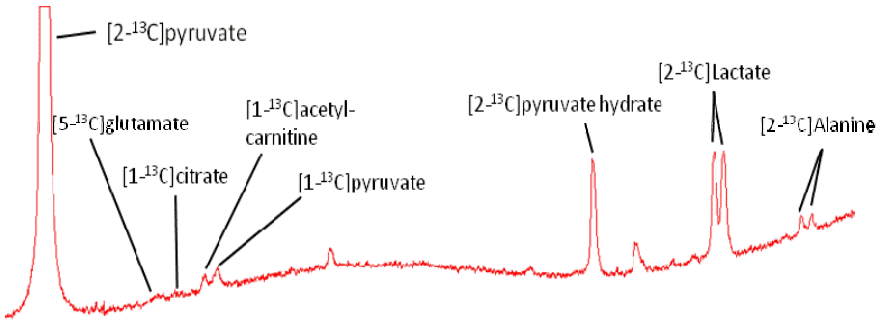

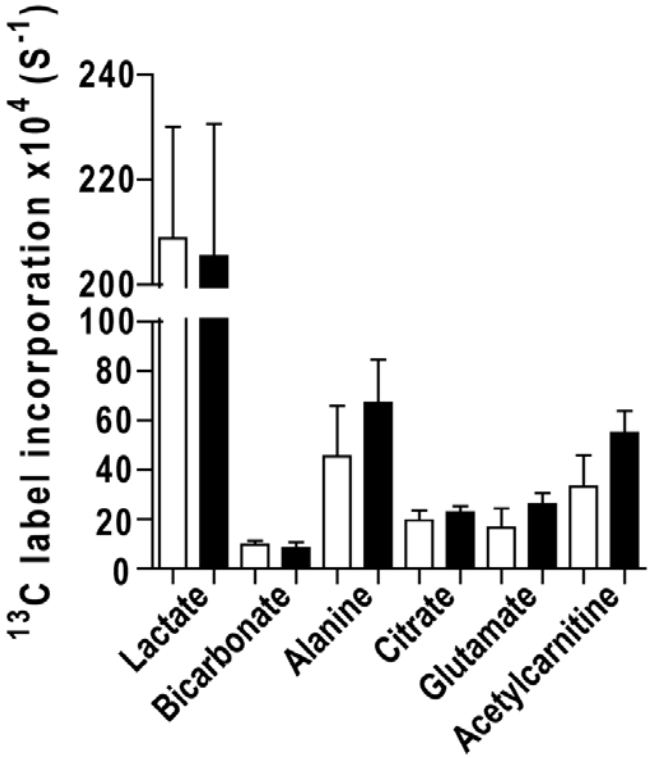

Figure S5 related to Figure 4

Left Panel: Representative sections from 2D-1H-13C-HSQC NMR spectra in the MetaboLab assignment tool for glutamate resonances (C2, C3, and C4) showing increased label incorporation in the C3 position for KO samples.

Right Panel: A. Concentrations of metabolites that were substantially altered in isolated hearts perfused with Krebs-Henseleit buffer containing 3- ^{13}C *–Glutamate. B. 3-* ^{13}C *incorporation to metabolites in isolated hearts perfused with Krebs-Henseleit buffer containing 3-* ^{13}C *–Glutamate. The glutamate was labelled at the C3 position as expected, the aspartate and pyruvate were labelled at the C2 and C3 positions.*

White: control, black: Fh1 KO; n=4/group, *p<0.05, **p<0.01.

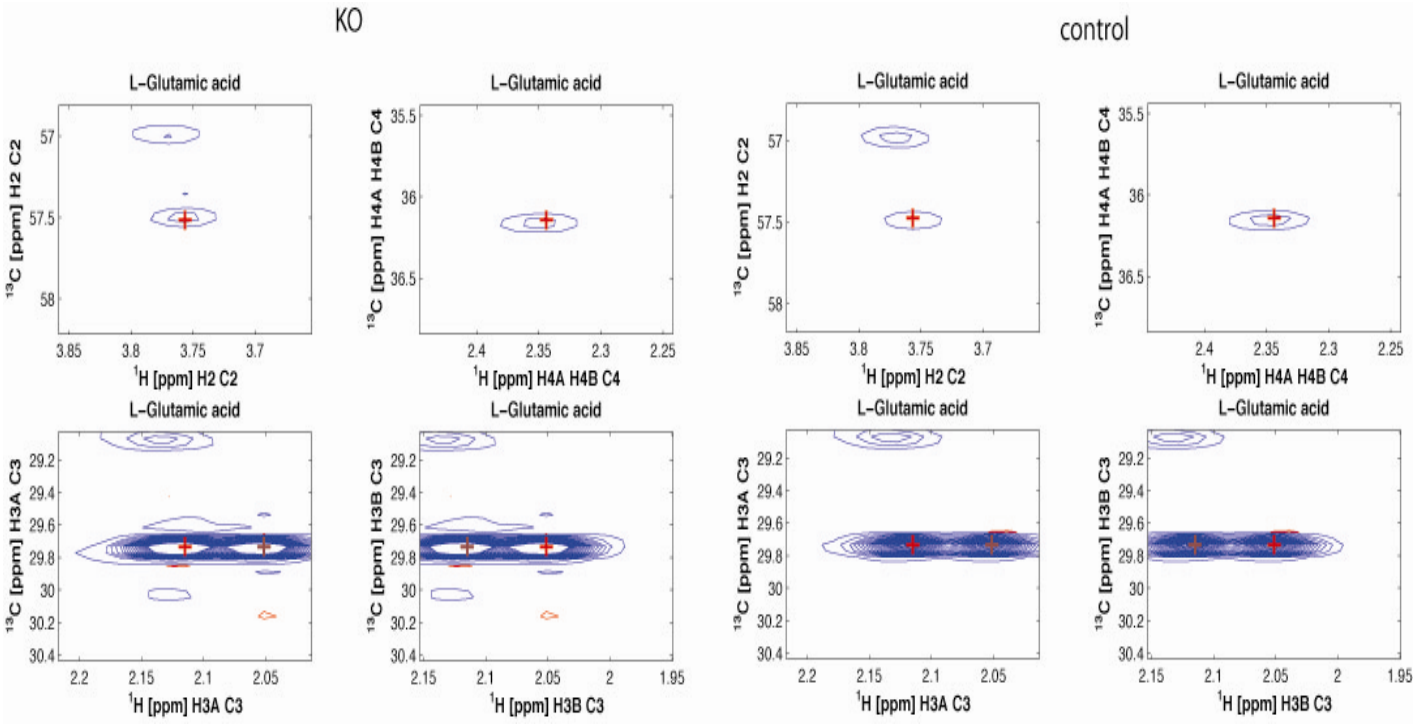

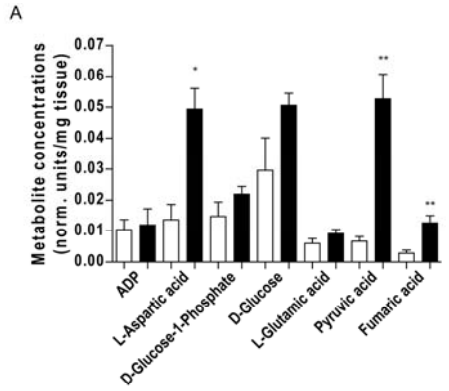

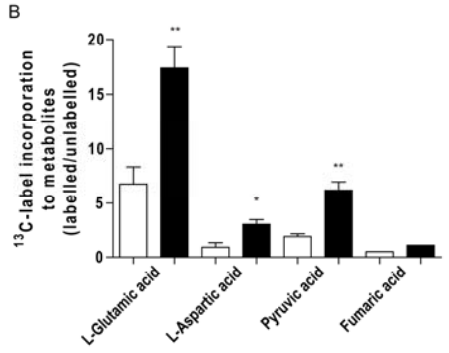

Figure S6 related to Figure 4

Glycolytic enzyme activity, respiratory complex activity and oxygen consumption are unaltered.

A. GAPDH activity, B. PGK activity, C. PK activity, D. Complex I. activity, E. Complex II-III. Activity, F. Complex IV. Activity, G. Pyruvate glutamate, H. Glutamate malate, I. Carnitine palmitoyl malate, J. Succinate rotenone. White: control, black: Fh1 KO; n=5/group * p<0.05.

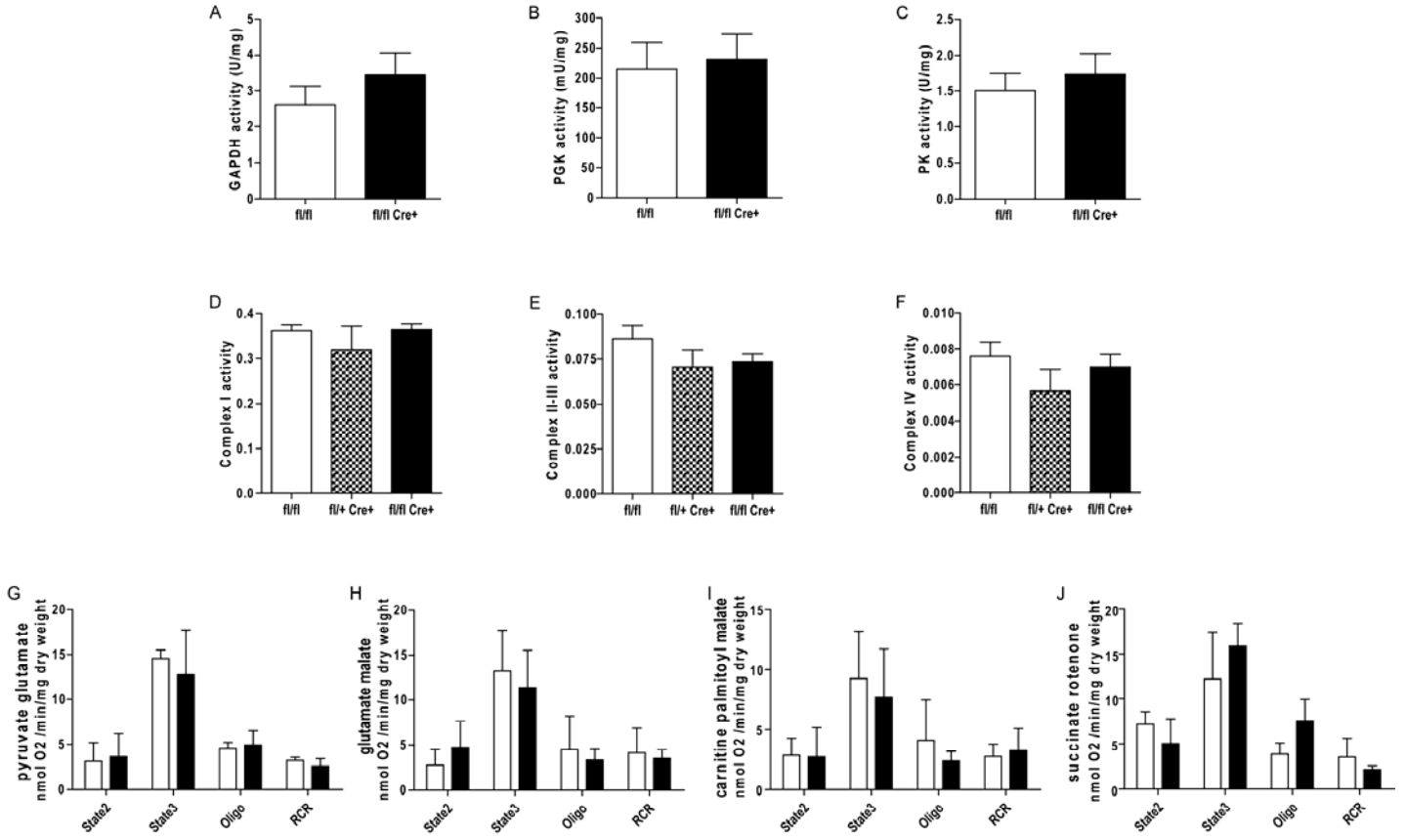

Supplemental Experimental Procedures

Two-dimensional echocardiography

2-D transthoracic echocardiography was performed under isoflurane anaesthesia (1–1.25%) using a Vevo 2100 Imaging System (VisualSonics, Toronto, Canada) with a 30 MHz linear array transducer on a bench-mounted adjustable heated platform with continual ECG monitoring. Ventricular dimensions and function were assessed from averaged measurements of at least three cardiac cycles using images obtained from the parasternal short-axis and long-axis views in accordance with consensus guidelines (Schiller et al., 1989). Image analysis was performed blinded to genotype off-line using Vevo software.

Left ventricular haemodynamics

A representative sample of mice fulfilling the above criteria was anaesthetized with isoflurane (1.25–1.5%) for the measurement of haemodynamic indices using a 1.4 F Millar Mikro-tip catheter (SPR-671) inserted into the LV via the carotid artery. After 15 min of baseline recordings, contractile reserve was assessed by infusion of dobutamine via the jugular vein (4–16 ng/g body wt/min) (Ten et al., 2005).

Perfused Heart Experiments

Mice were anesthetized with pentobarbitone (140 mg/kg body wt with 150 IU heparin, IP). Hearts were rapidly excised, cannulated, and perfused in Langendorff mode at a constant pressure of 80 mm Hg, 37°C with a modified Krebs-Henseleit buffer gassed with 95% O2/5% CO2 (pH 7.4) containing the following (in mmol/L): NaCl 118.5, NaHCO3 25.0, KCl 4.75, KH2PO4 1.18, MgSO4 1.19, D-glucose 11.0, and CaCl2 1.41. Susceptibility of FH-/- hearts to ischemia/reperfusion injury was tested by subjecting isolated hearts to 40 minutes of no-flow ischemia and 1 hour of reperfusion. All hearts had to fulfill the following inclusion criteria: coronary flow between 1.5 and 4.5 ml/ min, time from thoracotomy to aortic cannulation <3 min and no persistent dysrhythmia during stabilization. Coronary flow was determined every 5 minutes by

collecting effluent from the right ventricular outflow tract during 1 minute. After reperfusion hearts were stained with 1% 2,3,5 triphenyltetrazolium chloride (TTC) at 37˚C (pH 7.4), frozen and then sliced into 1 mm sections. Area of necrosis was assessed by computerised planimetry (Image-Pro Plus, MediaCybernetics, Bethesda, MD, USA), with measurements normalised against the weight of individual slices and final necrosis size expressed as a percentage of myocardial mass. To block heme oxygenase activity, 30 mg/kg zinc deuteroporphyrin 2,4-bis etylenglycol (ZnBG; Porphyrin Products) was administered to mice ip. once daily for four days preceding heart perfusion. ZnBG was dissolved in 50 mmol/l Na_2CO_3 to a final concentration of 1.4 mg/ml. The blocker solution was sterile-filtered, protected from light and before use adsorption was checked to exclude photodegradation (Czibik et al., 2009).

^{31}P MRS experiments were conducted on an 11.7 T (500 MHz) MR system comprising a vertical bore magnet (Magnex Scientific, Oxford, UK) and a Bruker Avance console (Bruker Medical, Ettlingen, Germany). A birdcage coil with an inner diameter of 10 mm (Rapid Biomedical, Wurzburg, Germany) was used as a transmit/receive coil for both phosphorus and proton frequencies. Following cannulation, the heart was lowered into the centre of the magnet and the position verified with scout images. After shimming, the water resonance line width was less than 50 Hz. Initially a single fully relaxed phosphorus spectrum was acquired for baseline analysis and correction of the spectra subsequently acquired under partially saturated conditions. Acquisition parameters were TR 10s, 60 averages, flip angle 90°, 10 kHz bandwidth and acquisition data size of 2048 points. Immediately following the completion of this scan, a series of partially saturated acquisitions were performed. Spectra were acquired every minute for 70 minutes. The acquisition parameters, chosen to optimize signal-to-noise ratio, included TR 0.25 sec, eight dummy scans, 232 averages, flip angle 35°, 10 kHz bandwidth and acquisition data size of 2048 points. As described above, the hearts were initially perfused at a normal flow rate for 10 minutes, followed by 30 minutes of global ischemia and then 30 minutes of reperfusion at the original flow rate. All spectra were fitted in the time-domain using the AMARES algorithm within jMRUI (Naressi et al., 2001a; Naressi et al., 2001b), with fits performed for phosphocreatine (PCr), inorganic phosphate (Pi) and adenosine tri-phosphate (ATP). Prior

knowledge used with the AMARES algorithm included specification of the J-coupling of the ATP peaks, approximations of the peak positions, and imposition of Lorentzian line shapes.

Mouse Acute MI model

12 hours following the final gavage, mice were subject to an acute myocardial infarction (MI) as described previously (Ahmet et al., 2009). Briefly mice were anesthetized with using isofluorane (3% v/v) and the chest cavity was opened. The left coronary artery was ligated at the level of left atrial apex. The chest and skin then was closed and the mouse was allowed to recover. 24 hours after the MI, the heart was perfused with 5% Evans Blue (Sigma), via an opening in the left ventricle, to distinguish the perfused area (blue staining) from the under-perfused area (no-staining).(Ahmet et al., 2009) Using a surgical microscope, the heart was isolated and cut into four pieces at the short axis and stained with 4% triphenyltetrazolium chloride (TTC, Sigma) for 30 min at 370C to distinguish the infarct area (unstained) from the area at risk (AAR; brick red stained) in the under-perfused area. The heart was then stored in 10% formalin and digitalized. All heart images were analyzed using NIH imagej software (http://rsb.info.nih.gov/ij/). The MI size was expressed as the percentage of dead area (unstained) to the total AAR (brick red). The surgeon and the MI assessor were blinded to the genotype and the treatments of the mice (the latter were randomised to DMF and vehicle). Data is expressed as the mean ± SEM. Comparisons were performed using a Students t-test, with p-values < 0.05 considered significant.

Microdialysis estimation of interstitial metabolite concentrations

In selected groups of the isolated perfused mouse heart study, we performed microdialysis for metabolic analysis. Following mounting of hearts in Langendorff mode, a microdialysis probe (membrane length 4 mm, cut-off 6 Da; AgnTho's AB, Sweden) was inserted into the LV free wall. Following implantation, a 20 min stabilization period was allowed for metabolites to reach equilibrium in the perturbed tissue. Perfusion fluid consisted of KHB solution deoxygenated with 95% N2 and 5% CO2. Perfusion velocity was 1 μL/min and the sampling time for each fraction was 10 min. Following separation in a Waters ACQUITY™ Ultra-performance liquid chromatography (UPLC) system (Waters Corp., Milford,

MA, USA), metabolites were quantitated using a Waters Xevo™ triple quadrupole tandem mass spectrometer (Waters Corp., Manchester, UK) with a Z-spray electrospray ionization source operating both in the positive and negative ion mode. All analytes were verified using two daughter ions when possible and deuterated internal standards for selected components. The final interstitial concentrations were calculated by correction for relative recovery rate: (citrate 27%, isocitrate 13%, malate 26%, fumarate 67%, succinate 26%, pyruvate 35%, α-ketoglutarate 26%, lactate 37 %, adenosine 41%, inosine 38%, hypoxanthine 38%, and xanthine 58%) measured during in vitro experiments at a flow of 1 µL/min (Birkler et al., 2010).

Cardiac myocyte isolation

Mice were weighed and anaesthetised with an intra-peritoneal injection of 20% pentobarbital (0.01 ml/g bw). Hearts were rapidly excised, cannulated *via* the aorta and perfused for 5 min at the constant pressure (100cm H_2O) with the Ca^{2+} free isolation buffer (mM: NaCl 130, KCl 5.4, $MgCl_2$ 3.5, Glucose 10, HEPES 5, $NaHPO_4$ 0.6 and Taurine 20; pH=7.4), gassed with 100% O_2 at 37°C. The perfusion medium was switched to an enzyme solution consisting of the isolation buffer and 1 mg/ml type II collagenase, 1.65 mg/ml BSA and 50µM Ca^{2+}. After 10 min, ventricular tissue was dissected, gently agitated in 2 ml of the storage buffer (mM: NaCl 120, KCl 5.4, $MgSO_4$ 5, Taurine 20, HEPES 10, Na-pyruvate 5, Glucose 20, $CaCl_2$ 0.2; pH =7.4), filtered through 25µm nylon gauze and centrifuged at 1000rpm for 5 min at room temperature, followed by the washes with PBS and snap-freezing.

Tissue harvest

All mice were weighed, euthanized by cervical dislocation, the heart excised, briefly washed with ice-cold PBS, blotted, and weighed before snap freezing in liquid nitrogen and storage at −80°C for further processing as described below.

Gene expression arrays

Total RNA was extracted from snap-frozen and pulverized heart tissue using the RNeasy Mini Kit (Qiagen, UK) following the manufacturers recommendations. Subsequent steps in the microarray expression processing and analysis were carried out by the Genomics and Bioinformatics Core Facilities at the Wellcome Trust Centre for Human Genetics.

Microarray Data Analysis

Gene expression data were obtained by hybridising a total of 10 samples from two experimental groups (n=5 per group) to Illumina MouseWG-6 Expression BeadChips. Raw data were exported from the Illumina GenomeStudio software (v1.6.0) for further processing and analysis using R statistical software (v2.11) (http://www.R-project.org) and BioConductor packages (Gentleman et al., 2004). Raw signal intensities were background corrected using array-specific measures of background intensity based on negative control probes, prior to being transformed and normalised using the 'vsn' package (Huber et al., 2002). Quality control analyses did not reveal any outlier samples. The dataset was then filtered to remove probes not detected (detection score <0.95) in any of the samples, resulting in a final dataset of 24,078 probes.

Statistical analysis was performed using the Linear Models for Microarray Analysis (limma) package. Differential expression between the experimental groups was assessed by generating relevant contrasts corresponding to the relevant comparisons. Raw p-values were corrected for multiple testing using the false discovery rate controlling procedure of Benjamini and Hochberg, adjusted p-values below 0.05 were considered significant. Significant probe lists were then annotated using the relevant annotation file (MouseWG-6_V2_0_R0_11278593_A) that was downloaded from the Illumina website (http://www.illumina.com) for further biological investigation. Gene set enrichment analysis methods (GSEA) are as described by Subramaniam and colleagues (Subramanian et al., 2005) and by Mootha and coworkers (Mootha et al., 2003), and were performed using web-based software (www.broad.mit.edu/gsea/).

Gene expression analysis

Quantitative reverse transcriptase–polymerase chain reaction (qRT–PCR) was used to detect mRNA levels of select target genes. One microgram of total RNA was reverse transcribed with High Capacity cDNA Reverse transcription Kit (Applied Biosystems) prior to amplification reactions performed using Fast Universal Master Mix on a StepOnePlus system (Applied Biosystems). Samples were run in duplicates in a total reaction volume of 10 µl. All Taqman oligos were inventoried products of Applied Biosystems. The relative quantities of target gene mRNA levels were normalized against the endogenous control beta actin, and relative expression was quantified using the comparative C_T method (User Bulletin #2; Applied Biosystems).

Immunoprecipitation of Keap-1

Immunoprecipitation of Keap1 was undertaken from whole myocardial lysates generated as previously described by homogenisation in RIPA buffer. Lysates were pooled by three in WT and KO groups. Preclearing of the lysates with irrelevant antibody (abcam ab6046 Rb IgG β-tubulin 0.01 µg/ml) and protein A sepharose (Sigma Aldrich, UK) 100 µl/ml, for 30 minutes under rotatory agitation, was undertaken to reduce unspecific protein A or immunoglobulin binding. Centrifugation followed for 10 min at 14000 g. The supernatant was recovered and Keap-1 antibody (Abcam ab66620, anti-Rb 1:10 dilution) added. Rotatory agitation followed for 1 hour. Protein A sepharose slurry was added at 70 µl/ml lysate, followed by rotatory agitation over night. The immunoprecipitate was centrifuged at 14000 g for 10 min and the supernatant discarded. The immunoprecipitate was resuspended in lysis buffer and subsequently centrifuged at. 14000g for 10 min. This was repeated three times. All steps until this point was performed on ice or in refrigerated spaces of ca 4˚C temperature. The final supernatant was discarded and the immunoprecipitate heated to 96˚C for 5 minutes in a single volume of double concentrated Laemmli loading buffer. The suspension was centrifuged at 14000 for 10 min and the supernatant recovered for SDS-PAGE.

Western blotting

SDS–PAGE and Western blotting were used for the detection of total or nuclear protein expression. Total protein extracts were prepared from approximately 20 mg of frozen, ground LV tissue. The pulverised heart was mixed with 300 µL of RIPA buffer (50 mM Tris-HCl [pH 7.4], 150 mM NaCl, 1% Triton X-100, 1% sodium deoxycholate, 0.1% SDS supplemented with protease inhibitor cocktail and PhosSTOP tablets [Roche]) and 0.5 mM phenylmethyl sulfonyl fluoride and sonicated for 2x30 seconds followed by passing the lysate through a 23 G needle 6 times and incubating for 1 hour at 4°C under constant agitation. The extract was centrifuged at 13000 rpm for 15 min at 4°C and the supernatant analysed for protein concentration using the Bradford protein assay (Biorad). Nuclear extracts were prepared as described previously with minor modification (Czibik et al., 2008). Briefly, hearts pulverised with mortar and pestle were resuspended in lysis buffer with a final concentration of 200 mM mannitol, 70 mM sucrose, 1 mM EDTA, 10 mM Hepes pH 7.5, protease inhibitor cocktail and PhosSTOP tablets [Roche] and 0.5 mM PMSF. Samples were centrifuged at 500g for 5 minutes. The pellet corresponds to the crude nuclear fraction that was immediately resuspended, and centrifuged at 5000g for 10 minutes in a buffer containing 10mM Hepes pH 7.5, 10 mM KCl, 0.1 mM EDTA, 0.1 mM EGTA, protease inhibitor cocktail and PhosSTOP tablets [Roche] and 0.5 mM PMSF. Samples were washed twice, first with the addition of Nonidet P-40. Finally, the pellets were incubated for 30 minutes with a buffer containing 20 mM Hepes pH 7.5, 400 mM NaCl, 1 mM of each EDTA and EGTA plus the same protease inhibitors and they were centrifuged at 14000g for 5 minutes. The supernatant was the nuclear fraction.

Equal amounts of protein (50 µg) were loaded onto 10% SDS–PAGE gels, which were run at 120 V for 2 hrs followed by transfer onto a PVDF membrane using an iBLOT system (Invitrogen). The membrane was blocked for two hours with 5% ECLadvance blocking agent and probed with rabbit anti-FH (Autogen Bioclear), anti-Keap1 (Abcam), anti-Hmox1 (Abcam) or goat anti-Nrf2 (Santa Cruz) primary antibodies in 1:1000 dilution followed by goat anti-rabbit-HRP or rabbit anti-goat-HRP secondary antibodies in 1:4000 (Abcam), respectively. To confirm equal loading of protein, the membrane was stripped of antibodies by incubating for 45 min in stripping buffer (2% SDS, 62.5 mM Tris–HCl, pH 6.8,

and 100 mM 2-mercaptoethanol) at 50°C, followed by staining with either rabbit anti-beta-tubulin (Abcam) or anti-H3 histone (Abcam) antibodies followed by goat anti-rabbit-HRP (Abcam). The antibodies were detected with either ECL or ECL Advance chemiluminescence kit (GE Healthcare, UK), visualized with a Biorad Chemi Doc XRS system and quantified with Quantity One software.

Biochemical analysis

Total creatine and total adenine nucleotide content was measured by HPLC as described previously with minor modifications (Neubauer et al., 1995) Frozen tissue was powdered with mortar and pestle in liquid nitrogen. 10-20 mg powder was homogenized in 0.4 N perchloric acid at 0°C and an aliquot of the homogenate was removed for protein determination. The homogenate was neutralized with KOH and centrifuged at 5500 rpm for 5 min at 4°C. The supernatant was used for the determination of high energy phosphates in relation to a standard. Protein concentration was measured by the Lowry method. Metabolite concentrations are expressed as nmol/mg protein.

Histology

Mouse hearts were cannulated through the aorta, rinsed with ice cold PBS followed perfusion with 4% paraformaldehyde for 2 min. Hearts were embedded in OCT compound. For a general overview of cardiac morphology, 10µm cryosections were stained according to Masson (Sigma) and visualized with a wide-field inverted Nikon TE2000U fluorescence microscope. To stain cell membranes, sections were incubated with Texas red-conjugated wheat germ agglutinin (Invitrogen) and visualized with a Zeiss 510 Metahead confocal fluorescence microscope.

Metabolite extraction for metabolomics analyses

Methanol and water were HPLC grade and were from Scientific and Chemical Supplies Ltd (Bilston, UK). Precellys homogeniser tubes were bought ready-filled from Stretton Scientific (Stretton, UK) and ammonium acetate and HPLC grade chloroform were purchased from Fisher Scientific (Loughborough, UK). Cardiac tissue from both WT (n=9) and FH -/- (n=9) was extracted in chloroform/methanol/water using a two

step protocol based on the method previously described by Wu et al.(Wu et al., 2008) Briefly, 60 mg (±5 mg) of cardiac tissue was taken for each mouse. Each sample was homogenised in 8 µl/mg methanol and 1.7 µl/mg water, using a Precellys-24 bead based homogeniser (Stretton Scientific, UK). Next, 8 µl/mg chloroform and 4 µl/mg water were added resulting in a final ratio of 2:2:1.6. The biphasic mixture was centrifuged and the upper polar layer removed and split into a 50 µl aliquot for mass spectrometry with the remainder retained for NMR analysis. After drying in a centrifugal concentrator (Thermo Savant, Holbrook, NY, US), all aliquots were stored at -80˚C prior to analysis. Quality control (QC) samples were also prepared by mixing 50 µl of the polar extracts from 8 different samples, and drying this solution in 100 µl aliquots prior to storage at -80˚C.

Metabolite analysis using FT-ICR mass spectrometry

Dried polar extracts were re-suspended in 150 µl (or 300 µl in the case of the QC sample) of an 80:20 methanol/water solution containing 20 mM ammonium acetate. The samples were analysed in negative ion mode using a hybrid 7-T Fourier transform ion cyclotron resonance mass spectrometer (LTQ FT Ultra, Thermo Fisher Scientific, Bremen, Germany) with a chip-based direct infusion nanoelectrospray ionisation assembly (Triversa, Advion Biosciences, Ithaca, NY). Nano electrospray conditions consisted of a 200 nl/min flow rate, 0.3 psi backing pressure and -1.7 kV electrospray voltage controlled by ChipSoft software (version 8.1.0). Mass spectrometry conditions included an automatic gain control setting of 5×10^5 and a mass resolution of 100,000. Analysis time was 2.25 minutes (per technical replicate) using Xcalibur software (version 2.0, Thermo Fisher Scientific) and data was collected over a mass range of *m/z* 70-590 using the SIM-stitching FT-ICR method detailed by Southam et al.(Southam et al., 2007; Weber et al., 2011) Each sample was analysed in triplicate. Nine QC samples were analysed prior to the analysis and a QC sample was analysed in triplicate every fifth sample.

Transient data (in the time domain) was collected and processed as described previously (Southam et al., 2007) using custom written code in Matlab (version 7.9.0, The MathWorks). Specifically, SIM stitching code2 (version 1.16) was used to join together all the SIM windows, to

reject peaks with a signal to noise ratio <3.5, and to internally calibrate the mass spectra using a list of 21 pre-defined metabolites. Next, a noise filtering algorithm(Payne et al., 2009) was applied such that only peaks that occurred in two (or more) of the three replicate measurements (per sample) were retained, and subsequently peaks were only retained if they were present in 50% (or more) of the cardiac samples. Finally, a K-nearest neighbour approach was used to substitute missing values, and the data was normalised using the probabilistic quotient approach(Dieterle et al., 2006) before undergoing the generalised log transformation according to the approach reported by Parsons et al.(Parsons et al., 2007) This resulted in a final peak matrix that consisted of a list of m/z values and their intensities across the samples.

Multivariate (PCA and PLS-DA) analyses were conducted on the dataset. For the PLS-DA, to discover those mass spectral signals that maximally separated the FH -/- from the wild type mice, a forward selection strategy based on regression coefficients was used. This required ranking the signals according to their absolute regression coefficients from the initial PLS-DA model (i.e. built using all signals), and then sequentially adding one signal at a time to a new list, rebuilding the PLS model for each case, until the classification error was minimised. Those signals contributing to the most discriminatory PLS-DA model were retained, and all other signals were rejected. The optimal PLS-DA model was cross validated using a venetian blinds approach with 4 splits. This approach was repeated 1000 times to achieve an "optimal model" classification error rate. To statistically evaluate this error rate and to be sure the model had not been overfitted, the class labels were randomly permutated and a new "permuted" model was built and cross validated in a similar way to give a "permuted" classification error rate. This permutation and model building process was also repeated 1000 times. Statistical significance of the prediction error for each class could then be calculated by comparing the optimal model classification error to the null distribution of permuted error rates. Specifically, a p value can be calculated by determining the number of instances where the permuted classification error is less than the optimal model error rate and dividing this value by the total number of permutations (in this case, 1000). A p value <0.05 was deemed to be of statistical significance.

Metabolite analysis using 1D ^{1}H NMR spectroscopy

Each polar fraction aliquot was resuspended in 55 µl of sodium phosphate buffer solution (0.1M, 90% H2O/10% D2O, pH 7.0) containing an internal chemical shift standard of 1 mM sodium 3-trimethylsilyl-2,2,3,3-d4-propionate (TMSP). Samples were sonicated in a bath (CAMLAB Transsonic T460) for 5 mins to achieve complete dissolution, with a cooling block added to the bath water to minimise sample heating. Next, samples were centrifuged for 10 mins at 21,885-g, and 50 µl of each supernatant was transferred to a 1.5 ml Champagne vial (8 mm diameter). 35 µl of each sample was transferred into a 1.7 mm NMR tube using a Gilson 215 liquid handler, controlled by the PrepGilsonST software package (Bruker Biospin, v1.2.80B). All tubes were capped and kept refrigerated at ca. 4°C until analysis.

Samples were analysed using a Bruker Avance III 600 MHz NMR spectrometer operating at 600.13 MHz ^{1}H resonance frequency, equipped with a 1.7 mm cryoprobe and SampleJet refrigerated automatic sample charger (Bruker Biospin, Coventry, UK). Automated tuning and matching was performed for each sample following 5 minutes post-insertion temperature equilibration at 298 K. 1-D 1H NMR spectra were collected using the standard Bruker pulse sequence noesygppr1d, which features NOESY pre-saturation water suppression during the relaxation delay, and spoil gradients. Pulse durations were optimised automatically for each experiment, with a typical 90° pulse duration being 9.4 µs. Other acquisition parameters include a spectral width of 7.2 kHz, relaxation delay of 3 s and 96 transients collected into 32,768 data points, requiring a 10 min acquisition time. Datasets were zero-filled to 65,536 points, and 0.3 Hz exponential line-broadening applied before Fourier transformation. All spectra were phased manually, baseline-corrected using a low frequency filter to remove the residual water signal, and calibrated (TMSP at 0.0 ppm) using TopSpin (version 3.0, Bruker). Processed spectra were imported into the Chenomx NMR suite software package (version 6.1, Chenomx, Edmonton, Canada) and further baseline correction was performed by fitting a cubic spline function through a series of defined spectral point, consistent for all samples, deemed to be baseline through visual inspection. For all samples, the concentrations

of metabolites giving rise to assignable NMR signals were calculated using Chenomx and its associated 600 MHz spectral library. These concentrations were corrected by multiplying each sample's concentrations by a normalisation scaling factor, obtained using Probabilistic Quotient Normalization4 (PQN) and custom-written Matlab scripts (Viant, 2003). Finally, t-tests were conducted within Matlab on each quantified metabolite.

For the isotopomer studies, isolated hearts were perfused with modified Krebs–Henseleit buffer as above with 1mM of [3-^{13}C] glutamate at 37°C. At the end of 45 minutes of perfusion, hearts were snap frozen in liquid nitrogen and metabolites extracted using the Precellys 24 system (Bertin Technologies). Samples were filled into 1.7mm NMR tubes using a Gilson 215 liquid handler as described previously. ^{1}H-^{13}C-HSQC spectra were recorded at 600MHz proton frequency employing a Bruker Avance II 600MHz spectrometer equipped with a crygenically cooled 1.7mm probe. 4096 increments were recorded for a sweep width of 160ppm in order to resolve the *J*-couplings between adjacent ^{13}C-atoms. In the direct dimension 1024 points were acquired, the sweep width was 13ppm. The retention time was 1.5s, 8 scans were acquired per increment yielding a total recording time of 7.5h for each HSQC spectrum. All 2D-spectra were analysed and signals integrated using the MetaboLab software (Ludwig and Gunther, 2011). MetaboLab facilitates the analysis of positional label incorporation by a spectra library in order to plot signals of individual atoms in metabolites, providing signal intensities for each metabolite. Signal intensities can be compared between the different atoms of each metabolite. We also compared with spectra of unlabelled control samples.

Mitochondrial Function Experiments

Saponin –permeabilized cardiac fibers isolated from the left ventricle endocardium were used to measure respiration of the total mitochondrial population in situ using a Clark-type oxygen electrode (Strathkelvin Instruments, UK) (Boudina et al., 2007; Kuznetsov et al., 2008; Khalid et al., 2011). A piece of myocardial tissue (~15mg) was cut from the endocardial free wall of the left ventricle with fine scissors and transferred to a pre-cooled Petri dish with ice cold relaxing and biopsy preservation solution (BIOPS) containing 10mM Ca2+-EGTA, 0.1 μM free Ca2+, 20

mM imidazole, 20 mM taurine, 50 mM K-MES, 0.5 mM DTT, 6.56 mM MgCl2, 5.77 mM ATP, 15 mM phosphocreatine, pH 7.1 (Veksler et al., 1987). Individual fiber bundles were separated with sharp forceps and permeabilized in BIOPS containing 50 mg/ml saponin for 20 min at 4°C .The presence of saponin perforated sarcolemma, while leaving the mitochondria morphologically and functionally intact (Kuznetsov et al., 2008). Permeabilized fibers were washed three times for 10 min in respiration medium containing (in mM): EGTA 0.5, MgCl2.6H2O 3, k-lactobionate 60, taurine 20, KH2PO4 10, HEPES 20, sucrose 110, fatty acid free-bovine serum albumin 1 g/l, pH 7.1 (Khalid et al., 2011). Individual bundles were transferred into respiration chamber containing air-saturated, continuously stirred respiration medium at 37°C. Mitochondrial respiration was assayed using pyruvate (10mM) with malate (5mM), glutamate (10mM) with malate (5mM), succinate (10 mM) with rotenone (0.5mM) and palmitoyl carnitine (40μM) with malate (5mM) (Boudina et al., 2007; Kuznetsov et al., 2008; Heather et al., 2010). Following the measurement of basal respiration (state 2), maximal ADP-stimulated (state 3) respiration was measured after addition of 2mM ADP. Postoligomycin (uncoupled, state 4) respiration was evaluated following the addition of oligomycin (1μg/ml) to inhibit ATP synthase (Lehman et al., 2008) or antimycin A in case of succinate stimulated respiration (Kuznetsov et al., 2008). Subsequently, fibers were removed, blotted and dried for 24h at 37ºC and dry weight recorded. The Strathkelvin 782 System v 4.4 software was used for data acquisition and analysis. Respiration rates are expressed as nanomoles of O2 per minute per milligram dry weight of fibers. Respiratory control ratios (RCR) were calculated as a ratio of state 3/state 4 respiration (Murray et al., 2008).

Enzyme Activity Assays

The myocardial enzymatic activities of glyceraldehyde- 3-phosphate dehydrogenase (GAPDH), 3-phosphoglycerate kinase (PGK) and pyruvate kinase (PK) were measured using coupled enzyme assays (Brindle and Radda, 1987; Ventura-Clapier et al., 1995; Knight et al., 1996; Dzeja et al., 1999) . Frozen, ground heart tissue (1mg/ml) was extracted with the buffer containing 150mM NaCl, 60mM Tris-HCl, 5 mM EDTA, 0.2% Triton-X 100, 1mM PMSF, 10ug/ml leupeptin, 1 ug/ml aprotinin, pH 7.5 for PK and PGK assay. Tissue extract for GAPDH assay was prepared

using 100 mM Tris-HCl (pH 7.6), 10mM glutathione reduced and 1mM EDTA extraction buffer. The pyruvate kinase activity was assayed at 30°C, 340nm in media containing 50mM imidazole (pH 7.6), 20mM KCl, 2mM MgCl2, 0.1mM EDTA, 0.1 mM NADH, 1mM ADP, 4.5 U/ml lactate dehydrogenase and 1mM phosphoenolpyruvate. The activity of glyceraldehyde-3-phosphate dehydrogenase was measured at 25°C, 340nm using reaction mixture containing 100 mM Tris-HCl (pH 8.6), 5 mM sodium arsenate, 3 mM dithriotreitol, 1.5 mM NAD+ and 1.5 mM glyceraldehyde 3 phosphate. 3-phosphoglycerate kinase activity was recorded at 25°C, 340 nm in the assay medium containing 50 mM imidazole buffer (pH 7.6), 2 mM MgCl2, 0.1 mM EDTA, 1mM ATP, 5mM 3-phosphoglycerate, 0.2 mM NADH. Mitochondrial complex activity was assessed as previously described (Ashrafian et al., 2010).

Immunofluorescence

HL-1 cells (a kind gift from Dr K. Gehmlich, University of Oxford, UK) were cultured in Claycomb medium (Sigma), supplemented with 10% fetal bovine serum (Sigma), 2 mM L-glutamine (Gibco), 100 U/mL penicillin, 100 μg/mL streptomycin (Gibco), and 100 μM noradrenaline (Sigma). Cells were incubated with dimethylfumarate (10 μM; Sigma) or vehicle (0.1% dimethylsulfoxide; Sigma) for 6 hours at 37deg C and then fixed with 4 % paraformaldehyde in phosphate buffered saline (PBS) for 5 minutes at room temperature. Cells were permeabilized with 0.2 % Triton X-100 in PBS for 5 minutes followed by incubation with anti-Nrf2 (1:50; Santa Cruz Biotechnology), diluted in 1 % bovine serum albumin in PBS, for 12 hours at 4 deg C. After washing with 0.1 % Tween-20 in PBS, cells were incubated with chicken-anti-goat IgG conjugated to Alexa Fluor 488 (Invitrogen). 4',6-diamidino-2-phenylindole (DAPI, Vector Labs) was used to visualise nuclei. Specimens were analyzed using a 63x/1.4 oil immersion lens.

Supplemental References

Ahmet,I., Spangler,E., Shukitt-Hale,B., Juhaszova,M., Sollott,S.J., Joseph,J.A., Ingram,D.K., and Talan,M. (2009). Blueberry-enriched diet protects rat heart from ischemic damage. PLoS. One. *4*, e5954.

Ashrafian,H., Docherty,L., Leo,V., Towlson,C., Neilan,M., Steeples,V., Lygate,C.A., Hough,T., Townsend,S., Williams,D., Wells,S., Norris,D., Glyn-Jones,S., Land,J., Barbaric,I., Lalanne,Z., Denny,P., Szumska,D., Bhattacharya,S., Griffin,J.L., Hargreaves,I., Fernandez-Fuentes,N., Cheeseman,M., Watkins,H., and Dear,T.N. (2010). A mutation in the mitochondrial fission gene Dnm1l leads to cardiomyopathy. PLoS. Genet. *6*, e1001000.

Birkler,R.I., Stottrup,N.B., Hermannson,S., Nielsen,T.T., Gregersen,N., Botker,H.E., Andreasen,M.F., and Johannsen,M. (2010). A UPLC-MS/MS application for profiling of intermediary energy metabolites in microdialysis samples--a method for high-throughput. J Pharm Biomed. Anal. *53*, 983-990.

Boudina,S., Sena,S., Theobald,H., Sheng,X., Wright,J.J., Hu,X.X., Aziz,S., Johnson,J.I., Bugger,H., Zaha,V.G., and Abel,E.D. (2007). Mitochondrial energetics in the heart in obesity-related diabetes: direct evidence for increased uncoupled respiration and activation of uncoupling proteins. Diabetes *56*, 2457-2466.

Brindle,K.M. and Radda,G.K. (1987). 31P-NMR saturation transfer measurements of exchange between Pi and ATP in the reactions catalysed by glyceraldehyde-3-phosphate dehydrogenase and phosphoglycerate kinase in vitro. Biochim. Biophys. Acta *928*, 45-55.

Czibik,G., Sagave,J., Martinov,V., Ishaq,B., Sohl,M., Sefland,I., Carlsen,H., Farnebo,F., Blomhoff,R., and Valen,G. (2009). Cardioprotection by hypoxia-inducible factor 1 alpha transfection in skeletal muscle is dependent on haem oxygenase activity in mice. Cardiovasc Res *82*, 107-114.

Czibik,G., Wu,Z., Berne,G.P., Tarkka,M., Vaage,J., Laurikka,J., Jarvinen,O., and Valen,G. (2008). Human adaptation to ischemia by preconditioning or unstable angina: involvement of nuclear factor kappa B, but not hypoxia-inducible factor 1 alpha in the heart. Eur J Cardiothorac. Surg. *34*, 976-984.

Dieterle,F., Ross,A., Schlotterbeck,G., and Senn,H. (2006). Probabilistic quotient normalization as robust method to account for dilution of complex biological mixtures. Application in 1H NMR metabonomics. Anal. Chem *78*, 4281-4290.

Dzeja,P.P., Vitkevicius,K.T., Redfield,M.M., Burnett,J.C., and Terzic,A. (1999). Adenylate kinase-catalyzed phosphotransfer in the myocardium : increased contribution in heart failure. Circ. Res. *84*, 1137-1143.

Gentleman,R.C., Carey,V.J., Bates,D.M., Bolstad,B., Dettling,M., Dudoit,S., Ellis,B., Gautier,L., Ge,Y., Gentry,J., Hornik,K., Hothorn,T., Huber,W., Iacus,S., Irizarry,R., Leisch,F., Li,C., Maechler,M., Rossini,A.J., Sawitzki,G., Smith,C., Smyth,G., Tierney,L., Yang,J.Y., and Zhang,J. (2004). Bioconductor: open software development for computational biology and bioinformatics. Genome Biol *5*, R80.

Heather,L.C., Carr,C.A., Stuckey,D.J., Pope,S., Morten,K.J., Carter,E.E., Edwards,L.M., and Clarke,K. (2010). Critical role of complex III in the early metabolic changes following myocardial infarction. Cardiovasc. Res. *85*, 127-136.

Huber,W., von,H.A., Sultmann,H., Poustka,A., and Vingron,M. (2002). Variance stabilization applied to microarray data calibration and to the quantification of differential expression. Bioinformatics. *18 Suppl 1*, S96-104.

Khalid,A.M., Hafstad,A.D., Larsen,T.S., Severson,D.L., Boardman,N., Hagve,M., Berge,R.K., and Aasum,E. (2011). Cardioprotective effect of the PPAR ligand tetradecylthioacetic acid in type 2 diabetic mice. Am. J. Physiol Heart Circ. Physiol *300*, H2116-H2122.

Knight,R.J., Kofoed,K.F., Schelbert,H.R., and Buxton,D.B. (1996). Inhibition of glyceraldehyde-3-phosphate dehydrogenase in post-ischaemic myocardium. Cardiovasc. Res. *32*, 1016-1023.

Kuznetsov,A.V., Veksler,V., Gellerich,F.N., Saks,V., Margreiter,R., and Kunz,W.S. (2008). Analysis of mitochondrial function in situ in permeabilized muscle fibers, tissues and cells. Nat. Protoc. *3*, 965-976.

Lehman,J.J., Boudina,S., Banke,N.H., Sambandam,N., Han,X., Young,D.M., Leone,T.C., Gross,R.W., Lewandowski,E.D., Abel,E.D., and Kelly,D.P. (2008). The transcriptional coactivator PGC-1alpha is essential for maximal and efficient cardiac mitochondrial fatty acid oxidation and lipid homeostasis. Am. J. Physiol Heart Circ. Physiol *295*, H185-H196.

Ludwig,C. and Gunther,U.L. (2011). MetaboLab--advanced NMR data processing and analysis for metabolomics. BMC. Bioinformatics. *12*, 366.

Mootha,V.K., Lindgren,C.M., Eriksson,K.F., Subramanian,A., Sihag,S., Lehar,J., Puigserver,P., Carlsson,E., Ridderstrale,M., Laurila,E., Houstis,N., Daly,M.J., Patterson,N., Mesirov,J.P., Golub,T.R., Tamayo,P., Spiegelman,B., Lander,E.S., Hirschhorn,J.N., Altshuler,D., and

Groop,L.C. (2003). PGC-1alpha-responsive genes involved in oxidative phosphorylation are coordinately downregulated in human diabetes. Nat Genet *34*, 267-273.

Murray,A.J., Cole,M.A., Lygate,C.A., Carr,C.A., Stuckey,D.J., Little,S.E., Neubauer,S., and Clarke,K. (2008). Increased mitochondrial uncoupling proteins, respiratory uncoupling and decreased efficiency in the chronically infarcted rat heart. J. Mol. Cell Cardiol. *44*, 694-700.

Naressi,A., Couturier,C., Castang,I., de,B.R., and Graveron-Demilly,D. (2001a). Java-based graphical user interface for MRUI, a software package for quantitation of in vivo/medical magnetic resonance spectroscopy signals. Comput. Biol Med *31*, 269-286.

Naressi,A., Couturier,C., Devos,J.M., Janssen,M., Mangeat,C., de,B.R., and Graveron-Demilly,D. (2001b). Java-based graphical user interface for the MRUI quantitation package. MAGMA. *12*, 141-152.

Neubauer,S., Horn,M., Naumann,A., Tian,R., Hu,K., Laser,M., Friedrich,J., Gaudron,P., Schnackerz,K., Ingwall,J.S., and . (1995). Impairment of energy metabolism in intact residual myocardium of rat hearts with chronic myocardial infarction. J Clin Invest *95*, 1092-1100.

Parsons,H.M., Ludwig,C., Gunther,U.L., and Viant,M.R. (2007). Improved classification accuracy in 1- and 2-dimensional NMR metabolomics data using the variance stabilising generalised logarithm transformation. BMC. Bioinformatics. *8*, 234.

Payne,T.G., Southam,A.D., Arvanitis,T.N., and Viant,M.R. (2009). A signal filtering method for improved quantification and noise discrimination in fourier transform ion cyclotron resonance mass spectrometry-based metabolomics data. J Am Soc. Mass Spectrom. *20*, 1087-1095.

Schiller,N.B., Shah,P.M., Crawford,M., DeMaria,A., Devereux,R., Feigenbaum,H., Gutgesell,H., Reichek,N., Sahn,D., Schnittger,I., and . (1989). Recommendations for quantitation of the left ventricle by two-dimensional echocardiography. American Society of Echocardiography Committee on Standards, Subcommittee on Quantitation of Two-Dimensional Echocardiograms. J Am Soc. Echocardiogr. *2*, 358-367.

Southam,A.D., Payne,T.G., Cooper,H.J., Arvanitis,T.N., and Viant,M.R. (2007). Dynamic range and mass accuracy of wide-scan direct infusion nanoelectrospray fourier transform ion cyclotron resonance mass spectrometry-based metabolomics increased by the spectral stitching method. Anal. Chem *79*, 4595-4602.

Subramanian,A., Tamayo,P., Mootha,V.K., Mukherjee,S., Ebert,B.L., Gillette,M.A., Paulovich,A., Pomeroy,S.L., Golub,T.R., Lander,E.S., and Mesirov,J.P. (2005). Gene set enrichment analysis: a knowledge-based approach for interpreting genome-wide expression profiles. Proc. Natl. Acad Sci U. S. A *102*, 15545-15550.

Ten,H.M., Chan,S., Lygate,C., Monfared,M., Boehm,E., Hulbert,K., Watkins,H., Clarke,K., and Neubauer,S. (2005). Mechanisms of creatine depletion in chronically failing rat heart. J Mol Cell Cardiol *38*, 309-313.

Veksler,V.I., Kuznetsov,A.V., Sharov,V.G., Kapelko,V.I., and Saks,V.A. (1987). Mitochondrial respiratory parameters in cardiac tissue: a novel method of assessment by using saponin-skinned fibers. Biochim. Biophys. Acta *892*, 191-196.

Ventura-Clapier,R., Kuznetsov,A.V., d'Albis,A., van Deursen,J., Wieringa,B., and Veksler,V.I. (1995). Muscle creatine kinase-deficient mice. I. Alterations in myofibrillar function. J. Biol. Chem. *270*, 19914-19920.

Viant,M.R. (2003). Improved methods for the acquisition and interpretation of NMR metabolomic data. Biochem Biophys Res Commun. *310*, 943-948.

Weber,R.J., Southam,A.D., Sommer,U., and Viant,M.R. (2011). Characterization of Isotopic Abundance Measurements in High Resolution FT-ICR and Orbitrap Mass Spectra for Improved Confidence of Metabolite Identification. Anal. Chem *83*, 3737-3743.

Wu,H., Southam,A.D., Hines,A., and Viant,M.R. (2008). High-throughput tissue extraction protocol for NMR- and MS-based metabolomics. Anal. Biochem *372*, 204-212.